Design and Development of a Baseline Deep Space Optical PPM Transceiver

Tsun-Yee Yan and Chien-Chung Chen
Jet Propulsion Laboratory
California Institute of Technology
4800 Oak Grove Drive, Pasadena, CA 91109

ABSTRACT

One of the NASA technology development program at the Jet Propulsion Laboratory aims to increase the information return capability while reducing the size of the spacecraft via **laser communications**. The deep space **optical transceiver** developed under this program employs **pulse position modulation (PPM)** for both uplink and downlink transmissions. An integral part of the **transceiver** is the development of signal acquisition and tracking subsystem. This paper describes the baseline design of the electronic assembly within the transceiver and modifications that are necessary for deep space communications. A two phase breadboard activity will be described to reduce technological risks associated with the development.

optical communications
pulse modulation

1. INTRODUCTION

Laser communication is an enabling technology applicable to future NASA near Earth and deep space missions that desire higher communications capacity than currently available by RF technologies. One of the NASA technology development program at the Jet Propulsion Laboratory (JPL) aims to increase the information return capability by at least an order of magnitude while reducing the size of the spacecraft. The technical merit of laser communications is derived from the fact that it offers a much higher collimated signal than conventional microwave. This super-collimated beam can result in a terminal design with greatly reduced size, mass and power requirements. Furthermore, laser communication systems are not susceptible to radio frequency interference and are not subject to frequency or bandwidth regulation.

Currently, data return from deep space missions is accomplished by direct space-to-ground link operating at S-, X-, or Ka-band. Planned deep space missions could demand return of vast quantities of scientific data either by direct link or through relays such as Mars missions. As more and more missions begin to operate at high downlink data rates to the DSN, resource and spectrum allocation and radio frequency interference (RFI) could become difficult to manage. Laser communications become a viable alternative to provide such a vast return.

There are several technical challenges that could hinder the development of deep space laser communications. First, the smaller transmit beamwidth imposes more stringent demands on the pointing accuracy of the instrument than near-Earth applications. Inaccurate beam pointing can result in significant signal fades at the ground receiving site and a severely degraded system performance. This is especially critical since the signal level will have much less link margin than near Earth scenario. As a result, the lasercom transmitter must be capable of maintaining tight residual pointing error within the transmit beamwidth. For typical deep space applications, this requires pointing budget to be on the order of a few microradians.

Second, current near-Earth laser communication system design uses cooperative laser beacon for high bandwidth line-of-sight pointing. As the communication distance between the spacecraft and the ground station increases, using beacon for acquisition and tracking becomes lass and less attractive. This is primarily due to the increasing demand on transmitting beacon power. A more attactive mode of providing a pointing reference is through the Sun-lit Earth as an pointing reference. Unfortunately, the tracking frame rate achievable at deep space must be slow enough to allow adequate photons to reach the image focal plane. In addition, the optical terminal must maintain pointing stability to counteract platform jitters from the spacecraft. This latter requirement translates into fast frame rate tracking similar to near-Earth applications. These seemingly conflicting requirements dictate the use of two control loops, one for transmitter stablization using fast frame rate. The other uses slow update rate for extended source tracking and acquisition. To further provide active control of the terminal, accelerometers are used to compensate real time platform jitter.

Third the terminal must be capable of stablizing the thermal requirements for the laser to maintain the linewidth and transmitting power. Other challenges include withstanding wider temperature ranges than near Earth applications, heavy radiation environment and operating within a few degree of Sun.

This paper is divided into five sections. Section 2 describes the design objectives, concept and overall mission scenario. Section 3 describes the functional block diagrams of the transceiver, including a description of any necessary changes from the laboratory OCD. Section 4 describes some open issues and risk areas.

2. DESIGN OBJECTIVES

The deep space optical transceiver will provide two way communications between the spacecraft and a ground station. The design objective was to deliver a flight qualifiable spacecraft terminal by 2001 with performance requirements shown in Table 2-1. This paper describes specific electronic designs related to the transceiver portion of the terminal. Current baseline considers a Q-switched Nd:YAG laser to produce short pulse width output using 256-ary Pulse Position Modulation (PPM) as the data modulation format for both uplink and downlink communications. Each PPM symbol frames occupies a total of $T_s=(256+N_d)T_l$ seconds. The number N_d is computed such that $1/T_s$ represents the laser pulse repetition frequency (PRF). Current design can support downlink data rate up to 60 Kbps for daytime operations and 100 Kbps for nighttime at a Sun-Earth-Probe angle of at least 2 degree and the distance of 6 AU. The uplink data rate is assumed to be limited to less than 2 Kbps although high rate telecommanding may be necessary for near-Earth applications.

TABLE 2-1. Performance Objectives for the transceiver

Item	Downlink	Uplink
Data Rate	up to 100 Kbps (60 Kbps, day)	up to 2 Kbps
Range	Up to 898 million km (6AU)	Up to 898 million km (6AU)
Transmit Wavelength	1.06 um	0.532 um
Transmit Aperture	30 cm	7 cm
System Mass	<15 kg	N/A
System Power Consumption	<50 W	N/A
Acquisition Scheme	Sun-lit Earth/Moon Beacon	Dowwnlink data/stellar ref.
Beacon Wavelength	Wideband	Narrrowband/wideband
Tracking Bandwidth	>100 Hz	>10 Hz
Acq Probability	> 0.999 in 10 s	> 0.999 in 60 s
Acq Probability of False Lock	< 0.001	< 0.001
Receiver Aperture	10 m	30 cm
Number of Channels	1	1
Bit Error Rate	7×10^{-3} (uncoded)	1×10^{-6}

Preliminary analysis for the planned Europa mission shows 3 dB link margin for both uplink and downlink at 6 AU as shown in Appendix A. The computation is based on the analytical tool FOCAS (Free-space Optical Communication Analysis Software) developed at JPL. The projected link performance shown in Table 2-1 assumes a 30 cm telescope on board spacecraft for both uplink and downlink communications with a baseline transmit power of 3 W for the downlink. The downlink link calculations assume a 3 implementation dB loss margin. The link analysis assumes an atmospheric transmission model consistent with that which is predicted using LOTRAN at the selected operating wavelengths. The downlink scintillation-induced fade is assumed to be small due to large aperture averaging. The receiver sensitivity is calculated by approximating the daylight sky irradiance with brightness of the full moon.

3. TRANSCEIVER DESCRIPTION

The development of the deep space transceiver follows a tight mission-like schedule for delivering of a flight-qualifiable instrument. Figure 1 shows the overall functional diagram of the PPM transceiver and its interfaces to other spacecraft components. The transceiver is divided into two major areas, Opto-mechanical Assembly (OMA) and electronics processing assembly (EPA). This paper describes the baseline design of the EPA which includes the transmitter, receiver, and pointing processing module. The design of the OMA is covered in a companion paper in this conference.

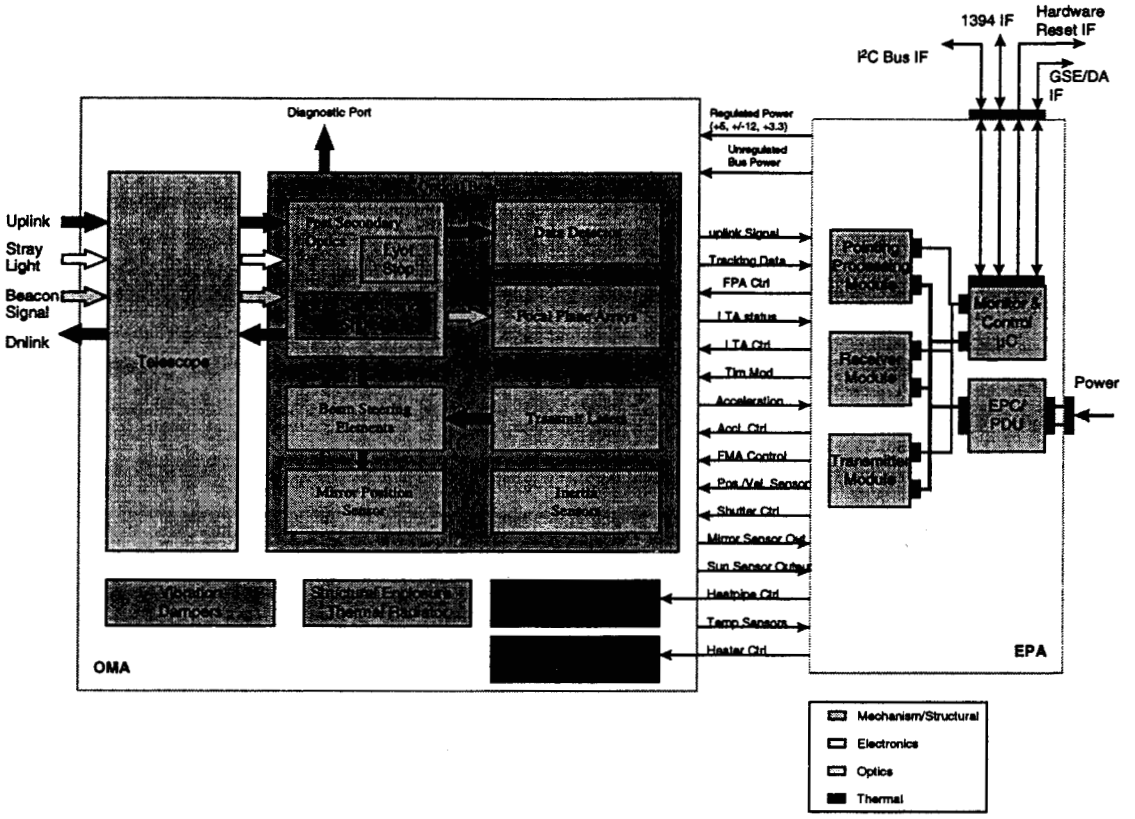

Figure 1. Optical Transceiver functional block diagram

The EPA assembly is envisioned to contain a stack of electronics and a set of laser driver modules. The electronic stack is designed to include 2 CPUs and occupy a stack of 4 circuit boards. Figure 2 shows the final packaging concept for the EPA at the spacecraft.

Due to heavy processing requirements for pointing, acquisition and tracking, one CPU is solely dedicated to perform these functions. The baseline transceiver design employs a TMS320C40 Digital Signal Processor (DSP) for the pointing and tracking function. A second processor is used to control transceiver operations and host interface. This second processor can be the X2000-supplied generic microcontroller. The targeted Application Specific Integrated Circuit (ASIC) will be prototyped using laboratory Field Programming Gate Arrays (FPGA) for digital portion of the transceiver and discrete component for the analog portion.

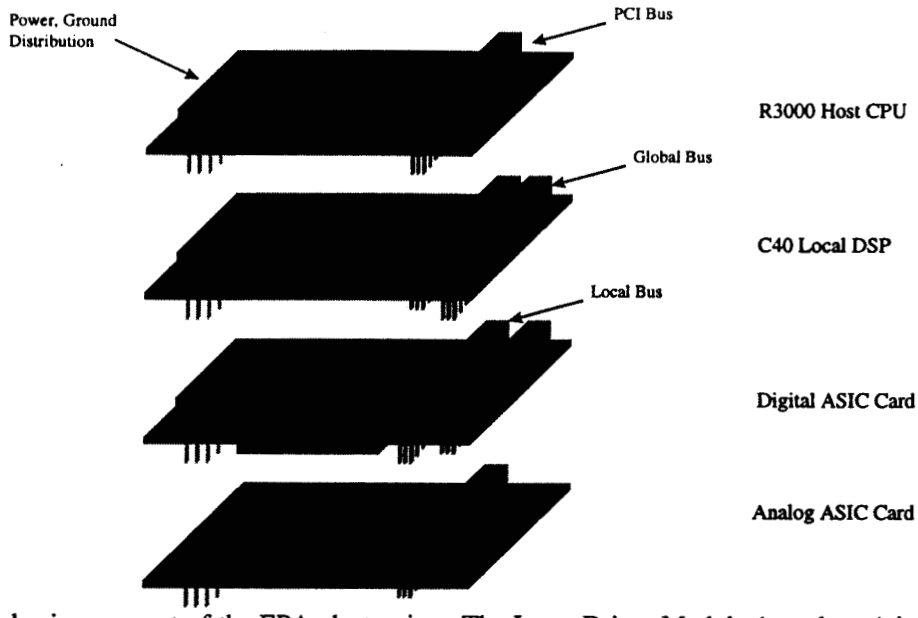

Figure 2. Packaging concept of the EPA electronics. The Laser Driver Module (not shown) is to be packaged along with the EPA, which may or may not be located on the OMA.

1. Monitor and Control MicroController

The subsystem and EPA relies on one of the microcontroller to perform subsystem monitor and control functions. This microcontroller will perform the following tasks:

1. Interface with spacecraft avionics for subsystem command and telemetry measurements. This function is performed over the high speed bus. At present, this is baselined as the IEEE 1394 firewire bus.
2. Interpret mode control commands and execute appropriate configuration of subsystem functions in response to the commands
3. Collect subsystem telemetry measurements and format the telemetry packet
4. Monitor sensor telemetry on the low speed bus (I2C bus)
5. Interface with the receive modules to control the uplink synchronization, decoding and uplink command interpretation functions
6. Interface with the transmit module to control the downlink encoding functions
7. Interface with the pointing processing module to collect status and to relay spacecraft provided attitude and point ahead data.

The monitor and control microcontroller is currently baselined as the X2000 provided generic microcontroller. The microcontroller, which can be implemented using a number of different processors, will interface with the rest of the EPA using a standard bus. A PCI bus is currently baselined by the X2000 avionics team.

2. Transmit and Receive Modules

The design of the transmit and receive modules follows the layered data format structure shown in Figure 3. The baseline design concept uses Reed-Solomon encoding and decoding to improve the end to end performance. The baseline selection of the Reed-Solomon (RS) code following CCSDS (Consultative Committee for Space Data System) recommendation for RF communications. Unlike the RF system, however, the optical system will not employ a convolutional inner code. A proposal has been accepted by NASA standards program to update the standard to include deep space optical communications using PPM beginning 1998.

For the optical link, the source data packets will be grouped into frames of 1115 bytes by the avionics (spacecraft C&DHS). The frame size is selected to match the standard, interleaving depth 5, (255,223) RS codes. The downlink frame data is then transmitted over the high speed bus to the lasercom subsystem. At the subsystem, the data is interleaved over a depth of 5 and then Reed Solomon encoded. A transfer frame header is then attached to each of the transfer frame. The transfer frame header will be used to denote start of transfer frame. Additionally, the transfer frame header will also be used for symbol timing recovery. This will be accomplished using either a special sync pattern or by using a correlation-type receiver which recognizes the work patterns.

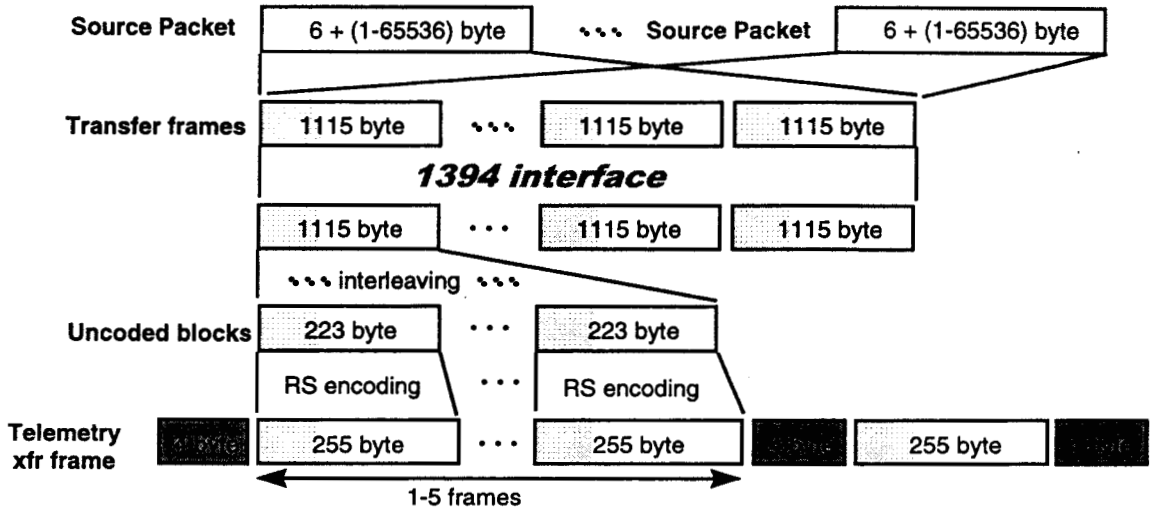

Figure 3. Layered telemetry format showing structure of a transfer frame, Reed Solomon encoding, and the source packets.

After encoding, the data is then modulated on the downlink using pulse position modulation (PPM) format. The transmitter module uses a fixed slot time period (25 ns), and controls the downlink data rate by modifying the amount of dead time between PPM data words. Figure 4 shows the prototype of the variable rate PPM transmitter module, excluding the Reed-Solomon encoder, suitable for both uplink and downlink laser control functions. The mean PRF can be selected between 95 Hz and 50 KHz. The FPGA design is achieved using the Xilinx XC6200 series FPGA. This device is embedded on a PCI (Peripheral Component Interconnect) PC board, and the design is downloaded during the execution of a program which communicates to the internal registers. Also shown in Figure 4 is the waveform generated from the FPGA for laser control functions at symbols 0, 1, and 255.

The uplink receiver is slightly more complicated. Figure 5 is the block diagram of the PPM receiver. An avalanche photodiode (APD) on the OMA converts the received optical signal into electronic pulses. After the optical PPM pulses are detected, a Automatic Gain Control (AGC) circuitry amplifies the signal and delays it by one slot time. The AGC regulates signal amplitudes and increases the dynamic range of the receiver tracking loop.

The signal will be threshold detected to aid the slot synchronization and control the operation of the phase lock loop. This threshold detection circuit is necessary because of the low average signal power to noise ratio of the optical link. Optical PPM obtains its performance by jamming the optical signal into a very narrow time slot such that, during the time slot, the signal to noise ratio is much higher than the average. An receiver synchronization loop operating without this threshold detector will therefore require a very narrow tracking loop when the data rate is low. This problem is particularly serious for uplink receiver where uplink data rates as low as 500 bps (62.5 pulse per second) can be expected. Without the threshold detector, therefore, the tracking loop will receive a small number (62.5 for a 500 bps link) updates per seconds, while having to operate over noise over the other periods. In order to obtain a reasonable tracking performance, therefore, loop time constant on the order of 1 hour will be needed. Such a narrow loop is clearly not feasible for deep space links. With the threshold detector, the receiver can now operate by gating the loop error signal. This will considerably reduce the acquisition time of the uplink to the order of minutes, even at low uplink data rates.

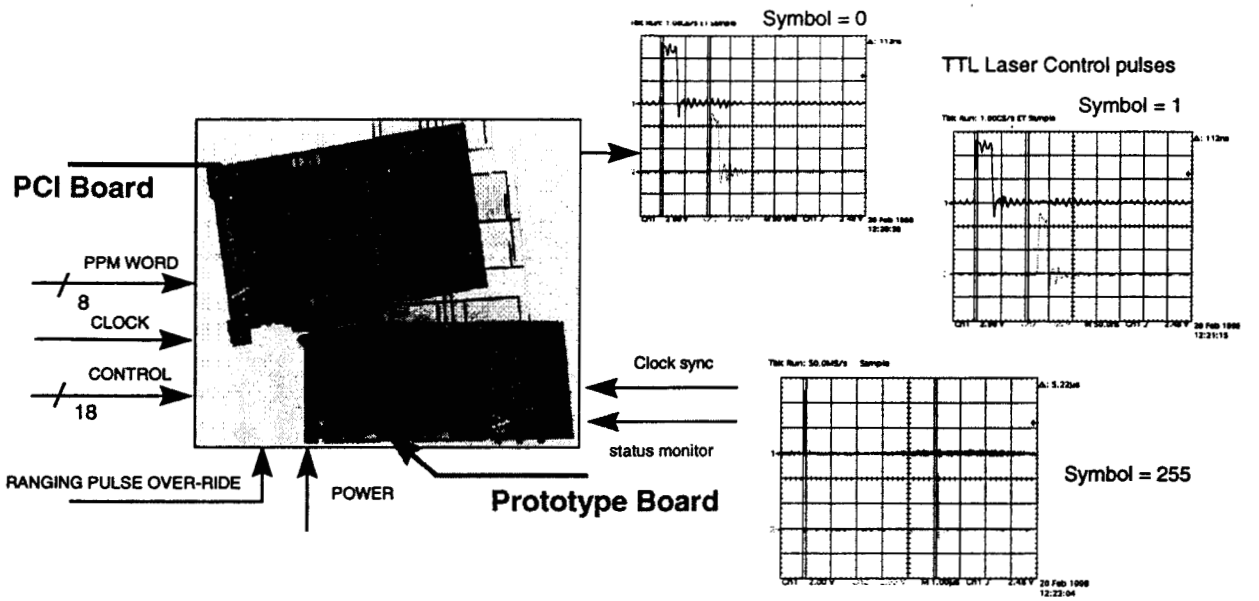

Figure 4. Prototype PPM mdulator currently being implemented as part of the end-to-end breadboard activity.

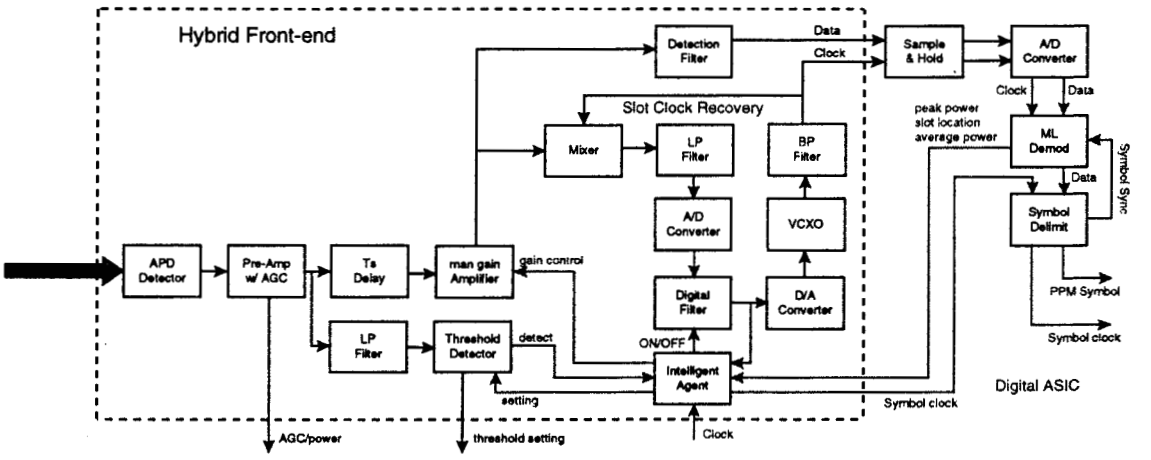

Figure 5. Block diagram of the PPM receiver to be incorporated as part of the EPA.

Note that since the receiver synchronization loop must operate at a very low signal to noise ratio. A small amount of transmit backscattering can cause the receiver to falsely lock onto the downlink slot period. Therefore, it is highly recommended that the transmit and receive time slot not be directly harmonically related. For the X2000 design, we have baselined a downlink slot period of 25 ns (40 MHz slot) versus a uplink slot period of 20 ns (50 MHz).

The recovered slot clock will be used for subsequent symbol and frame reconstructions. Under PPM, since the transmitter sends only one of 256 symbols in the time slot Ts. It has been shown [1] that under the maximum likelihood detection criterion, the receiver should select the largest value of the detector output after it is integrated synchronously within each slot. Theoretically, an integrate-and-dump circuit should be used to convert the analog signal to one digital sample per slot. For simplicity, a third order Butterworth Low Pass Filter (LPF) with 3 dB bandwidth of BTs=1.3 is selected

followed by a sample and hold. The performance degradation appears to be minimal based on preliminary simulation results. These slot values form the statistics from which PPM symbol synchronization can be derived.

Operations of the receiver is controlled by an Intelligent Agent (IA) hosted on the generic microcontroller (monitor and control □C). The CPU also controls the interface with the spacecraft through a 1394 firewire. The IA will adaptively adjust the threshold by monitoring the signal and noise statistics collected over a period of time. In addition, it "predicts" the arrival of the next signal pulse, thus reducing the false alarm probabilities and will significantly narrow down the time interval over which the threshold detector will operate. This also rejects spurious spikes that may happen during dead-time to masquerade as a valid signal.

The Intelligent Agent (IA) also has a built-in capability to determine, within a short time, the location of a given pulse within its symbol, and within the overall acquisition sequence. It further has the ability to generate an estimate for the time of arrival of the next pulse in the acquisition sequence based on prior data. Both of these information items, along with knowledge of the present status of the digital filter, are used within the rule-based system to selectively turn the digital filter on or off.

3. Pointing Processing Module

The second major module of the EPA is the pointing processing module. The design of this module represents an extension of the single steering mirror concept previously developed for OCD [2,3]

In the OCD a customized commercial Dalsa 128 by 128 CCD (Charge Coupled Device) camera was used to perform "windowed" read operation by clocking the vertical transfer lines of the CCD such that only lines containing the areas of interest will be read on a pixel-by-pixel basis; whereas other lines will be skipped without being read. Using a TI TMS32C40 DSP chip, the maximum achievable frame update rate is approximately 2kHz. This rate will be adequate for spacecraft platform jitter compensation but will be too fast for Sun-lit Earth beacon tracking. This is primarily due to the low flux density of the Sun-lit Earth at the distance of 6 AU.

Current design splits the functionality of the single tracking loop concept employed by the OCD by monitoring transmitted laser and beacon separately using two imaging devices. This dual loop tracking concept allows a slow frame imaging device monitors the Earth beacon while a fast imaging loop similar to OCD monitors the transmitting laser. Figure 6 shows a functional block diagram of this approach. The large format CCD array in OCD will be replaced by two individual pixel addressable Active Pixel sensors (APSs) [4]. Random access devices have shorter access time and hence has the potential of achieving even higher tracking bandwidth. Also shown in Figure 6 are three single axis accelerometers for platform monitoring.

Operations of the acquisition and control functions are performed by dedicated DSP processors. Several CPUs including R3000, PC603 series, and R6000 have been considered for radiation harden applications such as the planned Europa mission. Replacing TI TMS32C40 by any of the aforementioned processors requires rewriting approximately 8,000 lines of code, not to mention verification and testing. Recently two parallel DoD efforts have been devoted to bring radiation harden version of the TMS32C40 DSP chip available for space applications. JPL has enlisted with DoD as a potential government user once the chip becomes available. The targeted release date of December 1998 matches the year 2001 time frame of this technology development schedule. As a result, it has been decided to continue the development of the pointing processing module based on the TI DSP chips. This decision provides a number of advantages including well developed interactive object oriented software development environment matured under the OCD development and well trained software engineers on the DSP chip.

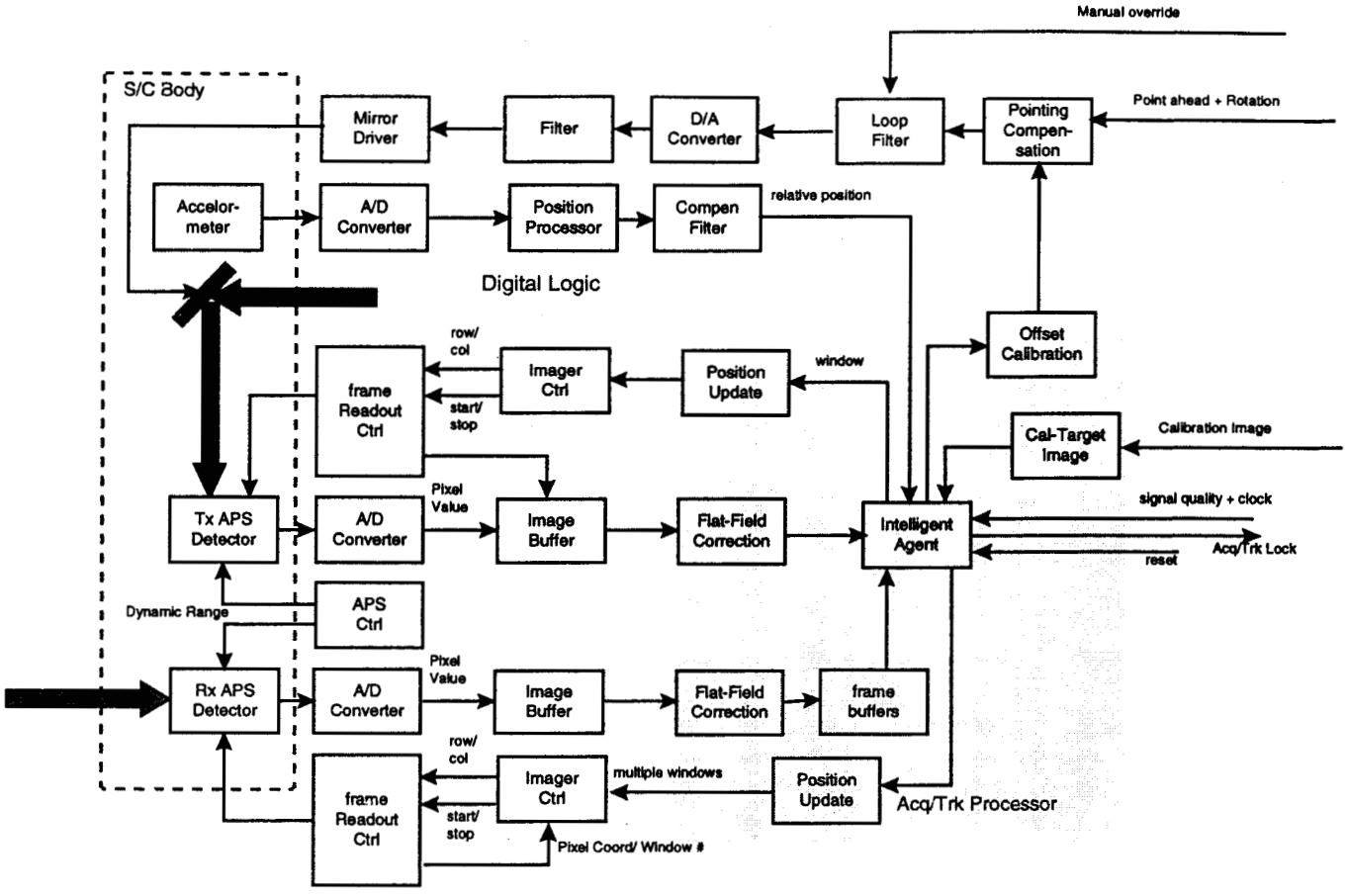

Figure 6. Block diagram of the pointing processing module showing the detector interfaces (to the celestial reference detector and the transmit reference detector), and the accelerometer interface

Since the pointing module will share a significant portion of the OCD design. The development effort will be largely depends on porting of existing OCD software to the new environment. It is estimated that another 8,000 lines of code in assembly and C development is necessary to complete the anticipated pointing, acquisition and tracking functions. Experiments run on existing OCD point source tracking software indicates that the TI TMS32C40 has over 50% idle time. Current software analysis indicates that a radiation harden C40 chip would be able to accommodate the anticipated functions. The additional functions will include individual test and diagnosis routines; device drivers for new devices such as APS, accelerometers,; augmented acquisition and tracking algorithm with multiple windows, selected region and extended source centroiding. Testing software will also be developed to characterize subsystem performance, statistical analysis, and stand-alone operation.

To reduce technology and program risk of the innovative dual tracking loop concept, a two phase engineering breadboard will be developed to validate the acquisition and tracking concept. Figure 7(a) and 6(b) show the block diagram of the breadboards. The objective is to demonstrate acquisition and tracking functions as well as end-end performance in the laboratory before final delivery and ASIC fabrication. The breadboard will leverage extensively on existing OCD acquisition and tracking hardware for the first phase of development. The second phase will procure flight qualifiable hardware for integrated testing with the transceiver. The JPL developed Laser Terminal Evaluation System (LTES) will be modified to accommodate the PPM transmitting and receiving functions.

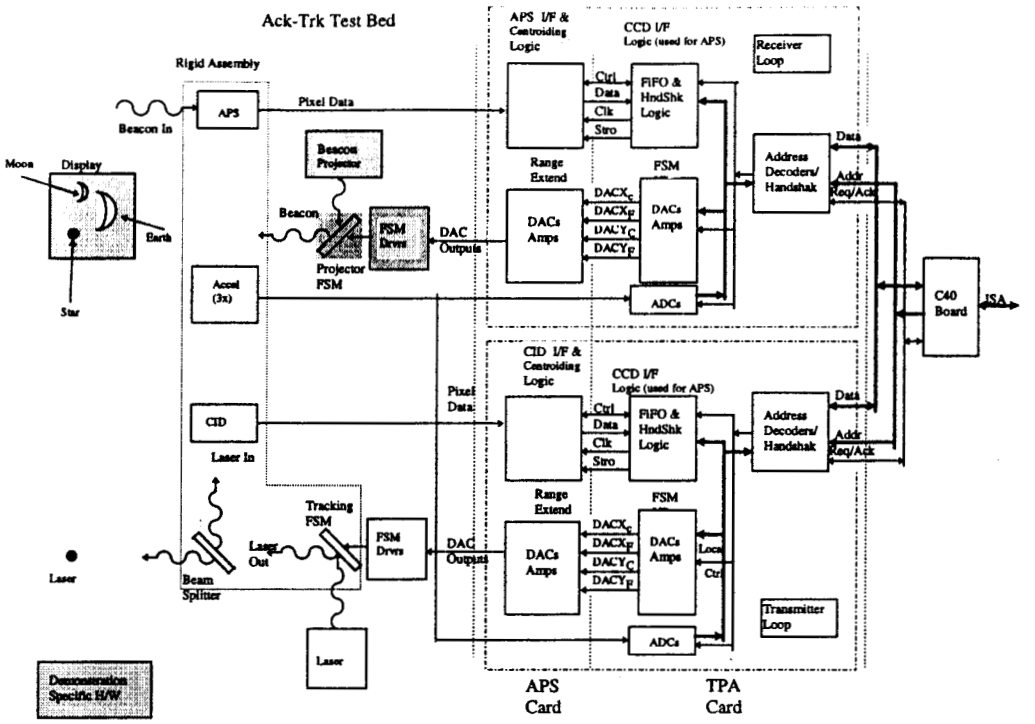

(a) Initial Acq-track breadboard concept

(b)

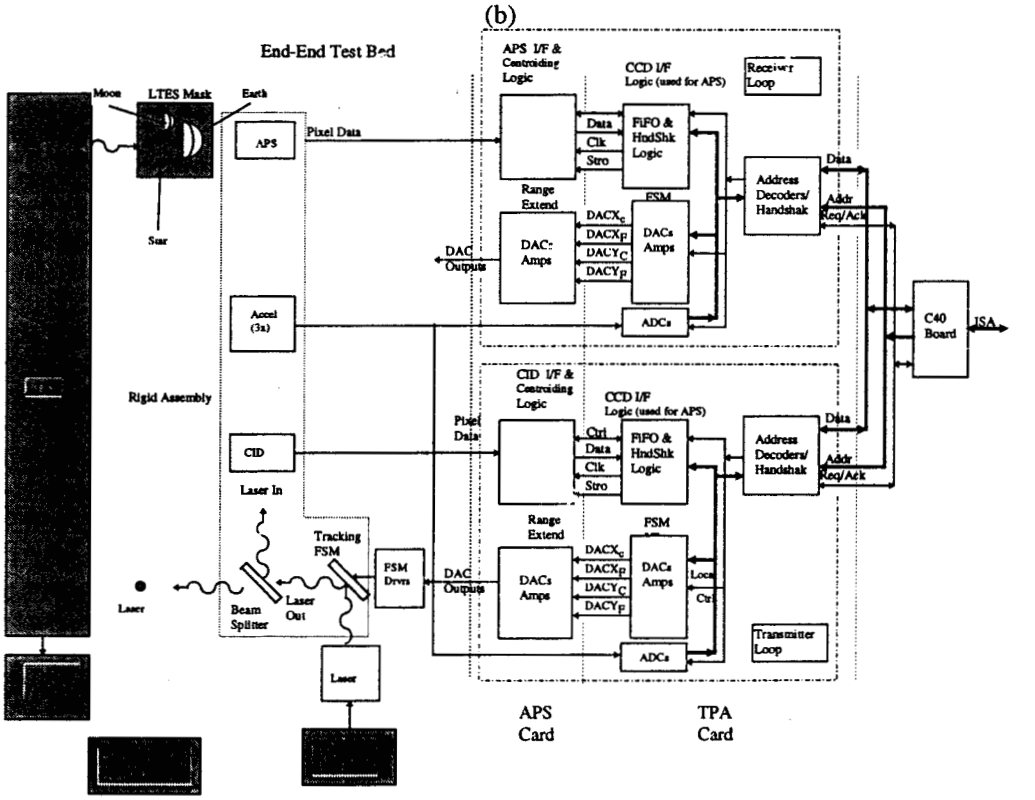

Figure 7. Concept of the demonstration breadboard evolution

4. SUMMARY

The transmitter, receiver, and pointing processing module of the deep space optical transceiver represents a departure from the OCD terminal which is designed primarily for near-Earth applications. It encompasses a significant technology improvement compared to near-Earth or crosslink lasercom system implementations. Two APS array detectors are used for transmitter and receiver loop pointing acquisition and fine tracking functions. An intelligent agent is conceived at the transceiver module to expedite the uplink acquisition time and improve the loop signal to noise ratio. Furthermore, a number of risk areas have been identified during the baseline design effort. By recognizing potential risk areas in the early stage of the development, the baseline design can tackle these items by validating concept using engineering breadboard. Currently the prototype receiver front-end has been developed to accommodate up to 50 KHz PPM pulses. The acquisition and tracking breadboard is under development.

5. ACKNOWLEDGMENTS

The research described in this report was carried out by the Jet Propulsion Laboratory, California Institute of Technology, under contract with the National Aeronautics and Space Administration. The authors would like to acknowledge the work of P. Arabshahi, D. Bean, A. Biswas, A. Del Castillo, P. Chi, M. Jeganathan, S. Lee, S. Monacos, M. Srinivasan, G. Stevens, H. Tsou, and V. Vilnrotter, for their contributions during various phases of the preparation of the article..

6. REFERENCES

1. V. Vilnrotter, M. Simon and M. Srinivasan, "The Optimum Decision Rule for PPM Signals with APD Statistics in the Presence of Additive Gaussian Noise", submitted to IEEE Transactions On Communications, April, 1998.
2. C. Chen, J. Lesh, "Optical Communications Demonstrator Instrument (OCDI) Requirements Document", JPL Report, September 1992.
3. Y. Yan, M. Jeganathan and J. Lesh, " Progress on the Development of the Optical Communications Demonstrator", OE-LASE'97, Jan 1997
4. E. R. Fossum, "Active-pixel sensors challenges CCDs," Laser Focus World, pp. 8387, June 1993.

APPENDIX A: UPLINK AND DOWNLINK DESIGN TABLES

Europa Downlink (Day, APD)

Link Summary

Link Range	**8.98E+08**	km	6.00 AU		
Data rate	**6.00E+01**	kbps	PPM (M = 256)		
Coded BER	**7.00E-03**		No Coding		
Transmit power	3.00	W average	20.00 kW (peak)	73.01	dBm
Transmit losses	68.4	% transmission		-1.65	dB
Transmitter gain	6.3	urad beamwidth		117.23	dB
Pointing losses				-2.01	dB
Space loss				-380.51	dB
Atmospheric losses	43.1	% transmission		-3.65	dB
Receiver gain	10.00	m aperture diameter		149.23	dB
Receiver optics losses	46.1	% transmission		-3.36	dB
Received signal	7.21E+02	photons/ pulse	6.74 nW (peak)	-51.72	dBm
Background signal level	3.98E+02	photons/ slot	2.97 nW		
Required singnal level	2.99E+02	photons/ pulse	2.79 nW (peak)	-55.54	dBm
Allowances and Adjustments				-1.00	dB
Link Margin				**2.82**	**dB**

Detailed Link Table

Laser (pulsed Q-switched Nd:YAG)					
Peak power			20.00 kW	73.01	dBm
Average power	**3.00**	W			
Wavelength	1.06	um			
Pulse width	20.00	ns			
Pulse width to slot width ratio	0.80				
Slot width or integration time	25.00	ns			
Dead time	0.13	ms			
Pulse repetition rate	7.50	kHz			
Transmit Optics					
Optics efficiency			**0.80**	-0.97	dB
Telescope (X2000)					
On-axis gain			5.29E+11	117.23	dB
Transmit beamwidth	**6.30**	urad			
Ideal beamwidth	6.30	urad			
Aperture diameter	**30.00**	cm			
Telescope optical losses			0.90	-0.46	dB
Loss from support structure			0.95	-0.22	dB
Pointing					
Allowance for pointing loss			**0.63**	-2.01	dB
Jitter (% of beamwidth)	**5.00**	☐			
Bias (% of beamwidth)	**5.00**	☐			
Mean loss (Airy beam pattern)	0.94				
Pointing-induced fade probability	0.00	☐			

Optics

Space loss			8.89E-39	-380.51	dB
Transmitter to receiver distance	6.00	AU			
Beam size at receiver location	0.89	Earth radii			
Atmospheric loss			0.43	-3.65	dB
Transmission at zenith	**75.00**	%			
Observation angle from zenith	**70.00**	deg			
Air mass	2.92				
Seeing at zenith	9.70	urad			
Telescope (10-m telescope)					
Gain			8.37E+14	149.23	dB
Aperture diameter	**1000.00**	cm			
Secondary obscuration	2.00	m			
Telescope F#	1.0				
Telescope losses			0.80	-0.97	dB
Relay Optics					
Filter loss			0.90	-0.46	dB
Acquisition/Tracking split loss			0.80	-0.97	dB
Loss due to redundant detectors			1.00	0.00	dB
Receiver pointing loss			1.00	0.00	dB
Detector truncation loss			1.00	0.00	dB
Other losses			**0.80**	-0.97	dB
Detector (EG&G SLiK APD)					
Quantum efficiency	38.00	%			
APD gain	39.08				
Detector diameter	1000.00	um			
Detector FOV	100.00	urad			
Amplifier (Transimpedance Model)					
Noise equivalent current (NEI)	0.34	pA/ sqrt(Hz)			
Detector/preamplifier bandwidth	25.00	MHz			
Peak power received at detector			**6.74 nW**	**-51.72**	**dBm**
Required power			**2.79 nW**	**-55.54**	**dBm**
Non-ideal bit synchronization				-1.00	dB
Pulse amplitude variations				-1.00	dB
McIntyre statistics (for APD)				1.00	dB
Code gain adjustments				**0.00**	dB
Allowance for atmospheric effects				0.00	dB
Link margin			**1.91**	**2.82**	**dB**
Pointing-induced fade probability	0.00	%			
Atmosphere-induced fade probability	0.00	%			

EG&G SLiK APD Detector with Transimpedance Model Amplifier

Detector quantum efficiency	0.38	
Detector ionization ratio	0.007	
Modulation extinction ratio	1.00E-06	
Required peak power	2.79	nW

Signal photons per pulse	299	photons
Phtons per bit	37	photons
Background Noise Power (see below)	2.97	nW
Bulk dark current	0.04	pA
Surface dark current	2.00	nA
Amplifier noise equivalent current (NEI)	0.34	pA/ sqrt(Hz)
Optimum gain	39.08	
Excess noise factor (ENF)	2.28	
RMS noise electrons (Kn)	381	electrons^2
(1-mer)*Ks/sqrt(2*mer*ENF*Ks+2*Kn)	4.12	a
SQRT(ENF*Ks+Kn)/SQRT(2*mer*ENF*Ks+2*Kn)	0.92	b
Value of integral in BER eq.	2.47	
BER (M-ary PPM)	7.01E-03	

Star in FOV	None	
Planet in FOV	None	
SkyCondition	Sunny1	
Average background power at detector	2.97	nW

a) Beamwidths refer to full width at 1/e^2 point

Europa Downlink (Night, APD)

Link Summary

Link Range	**8.98E+08**	Km	6.00 AU		
Data rate	**1.00E+02**	Kbps	PPM (M = 256)		
Coded BER	**7.00E-03**		No Coding		
Transmit power	3.00	W average	12.00 kW (peak)	70.79	dBm
Transmit losses	68.4	% transmission		-1.65	dB
Transmitter gain	6.3	Urad beamwidth		117.23	dB
Pointing losses				-6.02	dB
Space loss				-380.51	dB
Atmospheric losses	62.2	% transmission		-2.06	dB
Receiver gain	10.00	M aperture diameter		149.23	dB
Receiver optics losses	46.1	% transmission		-3.36	dB
Received signal	2.48E+02	Photons/ pulse	2.31 nW (peak)	-56.36	dBm
Background signal level	0.00E+00	Photons/ slot	0.00 pW		
Required singnal level	7.33E+01	Photons/ pulse	0.68 nW (peak)	-61.65	dBm
Allowances and Adjustments				-1.00	dB
Link Margin				**4.29**	**dB**

Detailed Link Table

Laser (pulsed Q-switched Nd:YAG)					
Peak power			12.00 kW	70.79	dBm
Average power	**3.00**	W			
Wavelength	1.06	Um			
Pulse width	20.00	Ns			
Pulse width to slot width ratio	0.80				
Slot width or integration time	25.00	Ns			
Dead time	73.60	Us			
Pulse repetition rate	12.50	KHz			
Transmit Optics					
Optics efficiency			**0.80**	-0.97	dB
Telescope (X2000)					
On-axis gain			5.29E+11	117.23	dB
Transmit beamwidth	**6.30**	Urad			
Ideal beamwidth	6.30	Urad			
Aperture diameter	**30.00**	Cm			
Telescope optical losses			0.90	-0.46	dB
Loss from support structure			0.95	-0.22	dB
Pointing					
Allowance for pointing loss			**0.25**	-6.02	dB
Jitter (% of beamwidth)	**5.00**	%			
Bias (% of beamwidth)	**5.00**	%			
Mean loss (Airy beam pattern)	0.94				
Pointing-induced fade probability	0.00	%			

Detailed

Space loss		8.89E-39	-380.51	dB

Transmitter to receiver distance	6.00	AU			
Beam size at receiver location	0.89	Earth radii			
Atmospheric loss			0.62	-2.06	dB
Transmission at zenith	**85.00**	%			
Observation angle from zenith	**70.00**	deg			
Air mass	2.92				
Seeing at zenith	9.70	urad			
Telescope (10-m telescope)					
Gain			8.37E+14	149.23	dB
Aperture diameter	**1000.00**	cm			
Secondary obscuration	2.00	m			
Telescope F#	1.0				
Telescope losses			0.80	-0.97	dB
Relay Optics					
Filter loss			0.90	-0.46	dB
Acquisition/Tracking split loss			0.80	-0.97	dB
Loss due to redundant detectors			1.00	0.00	dB
Receiver pointing loss			1.00	0.00	dB
Detector truncation loss			1.00	0.00	dB
Other losses			**0.80**	-0.97	dB
Detector (EG&G SLiK APD)					
Quantum efficiency	38.00	%			
APD gain	82.79				
Detector diameter	1000.00	um			
Detector FOV	100.00	urad			
Amplifier (Transimpedance Model)					
Noise equivalent current (NEI)	0.34	pA/sqrt(Hz)			
Detector/preamplifier bandwidth	25.00	MHz			
Peak power received at detector			**2.31 nW**	**-56.36**	**dBm**
Required power			**0.68 nW**	**-61.65**	**dBm**
Non-ideal bit synchronization				-1.00	dB
Pulse amplitude variations				-1.00	dB
McIntyre statistics (for APD)				1.00	dB
Code gain adjustments				**0.00**	dB
Allowance for atmospheric effects				0.00	dB
Link margin			**2.68**	**4.29**	**dB**
Pointing-induced fade probability	0.00	%			
Atmosphere-induced fade probability	0.00	%			
EG&G SLiK APD Detector with Transimpedance Model Amplifier					
Detector quantum efficiency	0.38				
Detector ionization ratio	0.007				
Modulation extinction ratio	1.00E-06				
Required peak power	0.68	nW			
Signal photons per pulse	73	Photon			

Phtons per bit	9	Photon
Background Noise Power (see below)	0.00	PW
Bulk dark current	0.04	PA
Surface dark current	2.00	NA
Amplifier noise equivalent current (NEI)	0.34	pA/sqrt-Hz
Optimum gain	82.79	
Excess noise factor (ENF)	2.58	
RMS noise electrons (Kn)	8	electrons^2
(1-mer)*Ks/sqrt(2*mer*ENF*Ks+2*Kn)	6.92	a
SQRT(ENF*Ks+Kn)/SQRT(2*mer*ENF*Ks+2*Kn)	2.22	b
Value of integral in BER eq.	2.47	
BER (M-ary PPM)	7.00E-03	

Star in FOV	None	
Planet in FOV	None	
SkyCondition	Dark	
Average background power at detector	0.00	pW

a) Beamwidths refer to full width at 1/e^2 point